Magnetic Nanoparticles Supporting Bio-responsive T_1/T_2 Magnetic Resonance Imaging

Connor M. Ellis [iD]**, Juan Pellico** [iD] **and Jason J. Davis** *[iD]

Department of Chemistry, University of Oxford, South Parks Road, Oxford OX1 3QZ, UK; connor.ellis@chem.ox.ac.uk (C.M.E.); juan.pellico@kcl.ac.uk (J.P.)
* Correspondence: jason.davis@chem.ox.ac.uk; Tel.: +44-(0)-1865-275914; Fax: +44-(0)-1865272-690

check for updates

Abstract: The use of nanoparticulate systems as contrast agents for magnetic resonance imaging (MRI) is well-established and known to facilitate an enhanced image sensitivity within scans of a particular pathological region of interest. Such a capability can enable both a non-invasive diagnosis and the monitoring of disease progression/response to treatment. In this review, magnetic nanoparticles that exhibit a bio-responsive MR relaxivity are discussed, with pH-, enzyme-, biomolecular-, and protein-responsive systems considered. The ability of a contrast agent to respond to a biological stimulus provides not only enriched diagnostic capabilities over corresponding non-responsive analogues, but also an improved longitudinal monitoring of specific physiological conditions.

Keywords: Bio-responsive; Nanoparticle; pH-responsive; Enzyme-responsive; Biomolecule-responsive; Magnetic Resonance Imaging; Diagnosis; Therapy; Mesoporous Silica Nanoparticles; Iron Oxide Nanoparticles

1. Introduction

Medical imaging is one of the most important tools available to a physician seeking to both diagnose and crystallise a prognosis. The modalities available for this are broad, primarily including magnetic resonance imaging (MRI), positron emission tomography (PET), computed tomography (SPECT), X-ray, and ultrasound (US). Of these, MRI constitutes the most convenient way of generating pathological detail at a deep tissue depth. Though now routine, MRI is inherently insensitive in generating contrast at specific incident imaging fields [1]. The use of a contrast agent during an MRI scan dramatically improves the sensitivity by interacting with local water protons and shortening their relaxation times [2–4]. The high surface area to volume ratio and chemical tunability of nanoparticles lead to high levels of potential functionalisation, with, for example, an improved biocompatibility upon tethering with polymers such as poly(ethylene glycol) (PEG) [2]. The sizes of particles can be modified to influence their route of clearance from the body, with small particles (<7 nm) rapidly cleared from the body via the kidney glomerulus. Nanoparticles that are larger in size are cleared by the reticuloendothelial system (RES), with the surface chemistry of the nanoparticles easily tuned to increase blood circulation times on chemical tethering. This provides a general marked improvement in relaxometric properties in comparison with their molecular analogues [5]. Biocompatible polymers, such as PEG, are used for this process, promoting a greater acquisition time and, hence, image quality. The ability of a contrast agent to respond to a specific biological stimulus is an invaluable diagnostic asset, with many diseases generating localised conditions that deviate from the standard background [6]. This can be accomplished by manipulating the sizes of particles to switch between the mode of contrast with the formation of nanoaggregates, as exemplified by pH-sensitive iron oxide systems. In addition, the choice of ligand can affect the responsive behaviour, where diffusive water access to the paramagnetic site can be manipulated by, for example, stimuli-responsive polymers

such as poly(acrylic acid), poly(L-histidine), or chitosan [7–10]. Alternatvely, molecular binding proteins can be incorporated onto the nanoparticle scaffold, promoting changes in contrast capabilities on recognition of a specific target, such as dopamine [11]. There has accordingly been much effort invested in the generation of contrast agents responsive to deviations in pH, biomolecular distribution, and enzyme activity (Table 1) [12,13]. These efforts will, therefore, provide the focus of this brief review. Physiologically-responsive MRI contrast agents are designed to switch "on"/"off" in response to a specific stimulus, as seen in Figure 1. In this example, there is a clear brightening of the phantom from the "off" state to the "on" state, thus providing an example of a T_1 responsive system. Alternatively, the system may be T_2 responsive, with an associated darkening in MRI contrast on stimulation or the agent may indeed be dual T_1/T_2 responsive, where the dominant mode switches depending on the local environment.
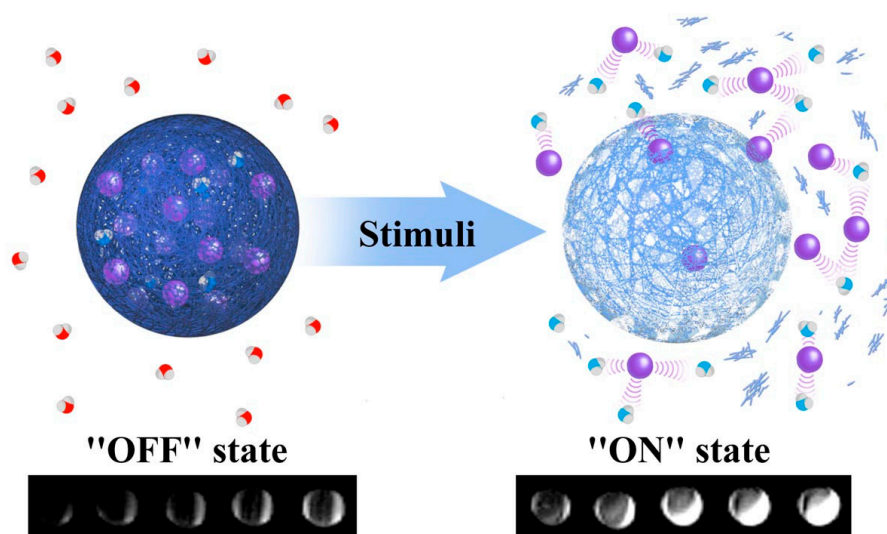
Figure 1. A schematic representing the impact of a generic stimulus on nanoparticle generated magnetic resonance imaging (MRI) contrast. The stimulus may be pH, enzyme activity, or temperature in nature, or may reflect the prescence of specific proteins/enzymes. In this example T_1 contrast capabilities are switched "on"/"off" with a particular biological stimulus. The MR active moieties (purple spheres) are encapsulated within a responsive matrix and released into solution in the presence of this particular stimulus (enhancing MR contrast by interacting with local water proton; red = non-enhanced relaxation, blue = enhanced relaxation). Adapted with permission from the authors of [13]. Copyright (2013) American Chemical Society.

2. MRI Theory

Water molecules are abundant within tissues, differing in concentration depending on the particular environment in which they reside. MRI operates by mapping the spatial distribution of the water protons to generate a 3D anatomical image of the pathological region of interest. In order to understand how effective a particular contrast agent is, one quantifies its concentration-dependent ability to shorten the longitudinal/transversal relaxation rates of water protons. If an external magnetic field is applied, the individual water proton spins align either parallel or antiparallel with the magnetic field, generating a net magnetisation along the principal, or longitudinal, axis. If a radiofrequency pulse is applied, this net magnetisation rotates away from the longitudinal axis into the perpendicular plane (inducing a net magnetisation). On removal of this pulse, the net magnetisation is recovered to the equilibrium state by two distinct processes, termed T_1 and T_2 relaxation. T_1, or longitudinal relaxation, characterises the recovery of the net magnetisation along the longitudinal axis, while T_2, or transverse relaxation, is the recovery within the transverse plane. The relaxation process that a particular contrast agent promotes has implications on the type of contrast generated, with T_1 contrast

agents brightening the physiological region of interest and T_2 darkening this region. The relaxation rate (R_i) can be calculated as follows:

$$R_i = \frac{1}{T_i} \qquad i = 1, 2, \tag{1}$$

where R_i corresponds to the relaxation rate, with the relaxation rate in the longitudinal axis denoted R_1 and that in the transverse plane denoted as R_2. This can then be used to calculate the relaxivity (r_i) if the concentration of the contrast agent is known:

$$r_i = \frac{\Delta R_i}{c_{CA}} \qquad \Delta R_i = \left[\frac{1}{T_{i,\, obs}} - \frac{1}{T_{i,\, water}} \right] \qquad i = 1, 2, \tag{2}$$

where r_i is the relaxivity, ΔR_i is the change in the relaxation rate between the observed and native water relaxation rates, and c_{CA} is the concentration of contrast agent. When $i = 1$, the longitudinal relaxivity is being considered, and the transverse relaxivity when $i = 2$. It is often useful to determine the relaxometric ratio (r_2/r_1) for a given contrast agent, because a larger relaxometric ratio corresponds to a greater r_2 contribution, and hence a more effective T_2 agent, with the reverse true for a T_1 agent.

Production of an effective stimuli-responsive contrast agent needs careful consideration of the parameters that govern relaxivity. The most significant factors affecting any switch in relaxivity are the hydration number (q), the rotational correlation time (τ_R), and the water residency time (τ_M) [14]. In general, the relaxation rate can be split into both inner sphere and outer sphere contributions (to the relaxivity), with the former directly proportional to q and given by the following equation:

$$R_1^{IS} = \frac{[CA]q}{55.6} \left(\frac{1}{T_{1m} + \tau_M} \right), \tag{3}$$

where R_1^{IS} is the inner sphere contribution to the relaxation rate, [CA] is the concentration of contrast agent, and T_{1m} is the longitudinal relaxation of the bound water to the contrast agent, with all other quantities previously defined [15]. As can be seen from Equation (3), increasing q will give a greater relaxation rate, and thus relaxivity. Commonly metal chelates are utilised as MRI probes as encorporation of the metal ion eliminates the associated toxicity of the free ion. By lowering the denticity of the metal associated chelate, q values can be increased, but this should be weighed against the loss in thermodynamic stability [14]. Ideally, the water residency time, τ_M, should be much shorter than the longitudinal relaxation of bound water for efficient relaxation ($\tau_M < T_{1m}$), but not so short that the water molecules do not undergo full relaxation on interacting with the paramagnetic chelate (otherwise exchange will take place before relaxation). Optimal vales are usually found in the order of 10 ns [16,17]. In addition to inner-sphere contributions, second-sphere and outer-sphere contributions are also important, with the distance of closest approach of outer-sphere water molecules (a) and the diffusional correlation time of outer-sphere water molecules (τ_D) influencing relaxivity [16]. A key contribution to relaxivity is the water access to the MR active site. This can be integrated into a designed responsive agent where, for example, stimuli-responsive polymers are incorporated into a nanoparticulate scaffold, with associated conformational changes in the polymer directly impacting water access to the paramagnetic centre (decreasing direct water access to the metal-chelate lowering the relaxivity). Increases in τ_R (slowing rotational motion) can be influenced by a change in the contrast agent aggregation state [18]. This is exemplified in work with iron oxide nanoparticles (IONPs), where irreversible changes in aggregation state cause a switch in contrast capabilities (between T_2 and T_1), as discussed in the next section of this review.

3. Bio-Responsive Magnetic Nanoparticles

3.1. pH-Responsive

The most common class of bio-responsive magnetic nanoparticles are those that respond to a change in local pH. Deviations in pH are prevalent in a wide variety of diseases, for example, cancer, inflammation, and Alzheimer's are all associated with decreased pH levels in local tissues [19,20]. pH-responsivity is achieved by several adopted approaches based largely on modulating water access to magnetic centres through, for example, the use of acid labile bonds (e.g., hydrazone linkages), pH-sensitive polymers (e.g., poly(acrylic acid) (PAA)), or structural decomposition by a disassembly process or degradation [21–24].

Iron oxide nanoparticles (IONPs) have been heavily employed in this context, with water access and aggregation switching being the primary responsive feature [25,26]. One such example involves the use of commercially available IONPs, where the carboxymethyl dextran coating has been loaded with doxorubicin (DOX) via electrostatic interactions [26]. Upon protonation of the dextran polymer in an acidic environment, the attractive electrostatic interactions between the positively charged DOX and the polymer are turned off, resulting in DOX release. The DOX presence was proposed to hinder the diffusion of water molecules within the coating of the particle, such that its release was then associated with greatly enhanced T_1 and T_2 relaxivities. As DOX is a chemotherapeutic agent, configurations such as this enable a dual-modal diagnosis and treatment.

A manipulation of IONP aggregation state can, as noted, also be exploited. Ordinarily, IONPs are T_2 active, however, the synthesis of small IONPs (< 20 nm) reduces this T_2 activity (and their saturation magnetisation) because of small magnetic domains within the particle [27–29]. Consequently, they function as T_1 contrast agents. The formation of aggregates within solution, however, results in a nanocomposite with a high saturation magnetization, and thus T_2 activity. One such example of such individual particle-nanocomposite switching has been through the incorporation of IONPs into a zeolitic imidazole framework (ZIF) to produce an Fe_3O_4-ZIF-8 assembly [30]. These disassemble under an acidic environment (pH < 6.2, Figure 2), releasing the individual IONPs, which function as a T_1 agent, whilst the initial Fe_3O_4-ZIF-8 assembly is T_2 active. Consequently, disassembly of the framework results in the irreversible switch from negative to positive contrast. The relaxometric ratio (r_2/r_1) for this system was specifically observed to decrease from $r_2/r_1 = 24.6$ at pH 7.4 to $r_2/r_1 = 5.7$ at pH 5.0 (indicating a strong progression towards T_1 performance). The same assemblies were also shown to disassemble in the presence of glutathione (overexpressed within the tumour site), indicating additional redox-responsiveness. Another method of incorporating IONPs into a nanocluster assembly relies on an i-motif linker [31]. I-motif DNAs undergo a structural change with pH, causing dissociation of the nanocluster assembly under conditions of low pH. Again, a change in contrast capabilities from T_2 to T_1 is observed as individual IONPs are released, with the relaxometric ratio decreasing significantly from $r_2/r_1 = 63.3$ at physiological pH to $r_2/r_1 = 7.1$ at pH 5.5. The self-assembly of IONPs containing pH-responsive ligands has similarly been reported to produce pH-sensitive magnetic 'nanogrenades' (PMNs) [32]. These contain imidazole functional groups providing pH-sensitivity (imidazole pK_a ~ 6.8), catechol groups to facilitate the self-assembly (catechol having a high affinity for the IONP surface), and phenyl entities to control the hydrophobicity of the particles. Within a tumour microenvironment (~pH 6.8), the imidazole groups protonate and electrostatically repel, the hydrophobic interactions weaken, and complete dissociation into individual IONPs occurs. This process is accompanied by a markedly more efficient T_1 relaxation. A similar approach has also been applied using hydrazine cross-linked IONP nanocluster assemblies [25]. As pH decreases, the hydrazone linkages hydrolyse (pH 5.5), releasing individual IONPs, and greatly amplifying the T_1 contrast. This is reported in work by Li et al., where $r_2/r_1 = 33.8$ at physiological pH and 4.2 at pH 5.5 [25].
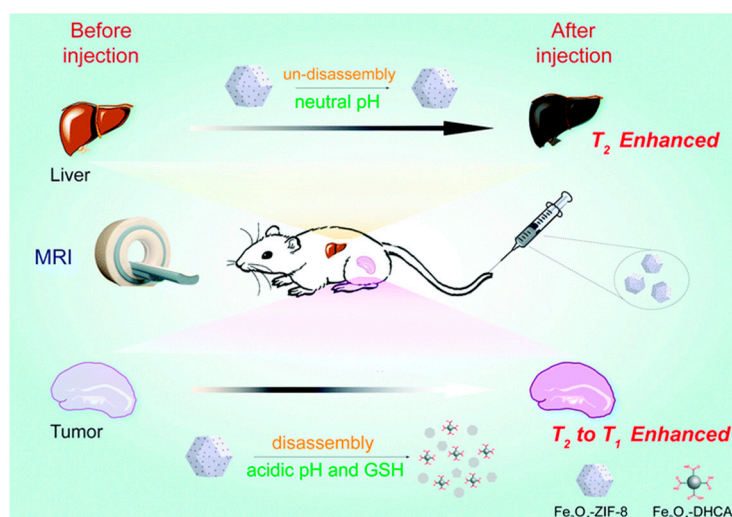
Figure 2. A schematic showing how the incorporation of iron oxide nanoparticles (IONPs) into a pH-responsive zeolitic imidazole framework (ZIF-8 moiety) can engender a responsive contrast capability. At neutral pH, the nanocomposite remains intact, with T_2 contrast exhibited. On decreasing pH, the ZIF-8 structure disassembles switching from T_2 to T_1 contrast capabilities. This framework was shown to be similarly responsive to glutathione (GSH). Reproduced from the work of [30] with permission from The Royal Society of Chemistry.

Mesoporous silica nanoparticles (MSNs) were first reported in 1992, building on the original synthesis of silica nanoparticles by Stöber et al. in 1968 [33,34]. The mesoporous nature, achieved by the use of a surfactant template, paved the way for their use in a vast range of applications, including contrast agents for drug delivery, multi-modal imaging, and MRI [35–37]. The latter has been achieved by doping the MSNs with paramagnetic ions, often by functionalisation with Gd-containing macrocycles [38].The porous nature is attractive, as functionalisation of Gd-chelates in the outer pore channel produces nanoparticles with greater relaxivities than corresponding non-porous analogues. This has been ascribed to the confinement effects around the Gd-chelate that favourably reduce water exchange/tumbling rates, while retaining facile access to the bulk water. By further expanding this platform, bio-responsivity can be accomplished, with one of the first reported examples of this using MSNs in combination with external surface protein recognition to reversibly gate T_1 contrast capabilities [39].

The functionalisation of MSNs with polymers containing ionisable groups introduces a generic pH-responsivity that has been utilised in gatekeeper switching based drug release. Polymers such as poly(vinyl pyridine) (PVP), chitosan, poly(acrylic acid) (PAA), and poly(L-histidine) (PLH) have all been applied on MSNs for this purpose [7–10]. Recently, Gd-chelates have been incorporated into MSNs capped with the pH-responsive polymer PAA to produce a pH-responsive nanoparticulate T_1 contrast agent (Figure 3) [40]. The pH-responsivity here arises from the protonation state of the monomer unit and associated polymer conformational change from a hydrophobic, collapsed conformation to a hydrophilic, extended conformation as it charges. With the polymer in its extended state, the improved water access through the pore channels leads to a reversible 130% increase in r_1 values (Figure 3c). This work constitutes the first reported example of a fully reversible pH-responsive nanoparticulate T_1 contrast agent.
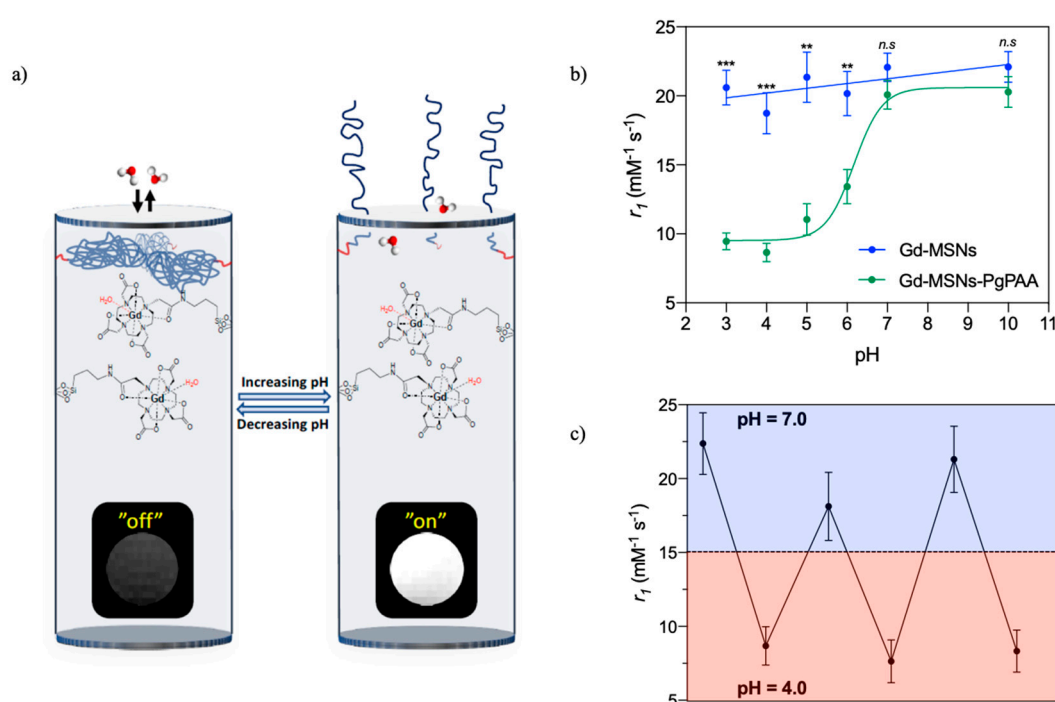
Figure 3. (**a**) Schematic representing a pH-responsive, reversible capping of the pore channels of a mesoporous silica nanoparticle (MSN) with poly(acrylic acid) (PAA) (blue polymer chains). The associated change in MR contrast is also shown. (**b**) A graph detailing the change in relaxivity with pH. (**c**) The reversible relaxivity switching with pH. Adapted from the work of [40] with permission from The Royal Society of Chemistry.

The integration of manganese oxide into MSNs can also be used to produce T_1 active particles. If embedded in hollow MSNs, the manganese oxide can be reduced in an acidic environment releasing paramagnetic, T_1 active Mn^{2+} ions [41]. These particles have been shown to exhibit an 11-fold increase in relaxivity as solution pH decreases from pH 7.4 to pH 5.0. In addition, the hollow MSN scaffold provides a multi-modal imaging ability, as the hollow interior is effective at amplifying sound, and thus returning an ultrasound signal. Manganese has also been combined with the IONP scaffold to produce pH-sensitive contrast agents. This is exemplified in work by Duan et al., where MnO_2 nanosheets were imbedded into carbon coated IONPs to produce dual-modal T_1/T_2 magnetic nanoparticles [42]. IONPs within the core support T_2 contrast acquisition, whilst the degradation of the MnO_2 nanosheets in an acidic microenvironment (releasing Mn^{2+}) promote a switch to a dominant T_1 response.

3.2. Biomolecule-Responsive

An image contrast responsive to the presence of specific biomolecules or ions can be a potent means of imaging localised biological activity. For example, Ca^{2+} is important in cell signalling and Zn^{2+} is vital in cellular physiology [43,44]. Neurotransmitters, such as serotonin, dopamine, oxytocin, and acetylcholine, are vitally important in regulating chemical communication within the brain and have also been of focus in responsive imaging [11,45]. The development of IONPs for which the magnitude of the transversal relaxivity responds to dopamine and serotonin has, for example, been reported by Hsieh et al. (Figure 4) [11]. In this work, two types of IONPs were synthesised, one functionalised with a dopamine binding protein (BM3h), and the other an analogue with the ability to compete with dopamine for protein binding (Tyr-PEG). In the absence of dopamine, these complementary IONPs bind together, forming clusters of particles with a high r_2 value. However, in the presence of dopamine, a potent competitor, inter-particle binding is impaired, resulting in a disassembly of the composite and an associated decrease in r_2. A similar architecture, modified for a serotonin response, was additionally developed. The same group also reported Ca^{2+} sensitive IONPs that

undergo a similar, but reversible aggregation mediated by an IONP surface coating with synaptotagmin. The synaptotagmin monomer has two binding sites for Ca^{2+}, with IONP aggregates forming in the prescence of Ca^{2+} promoting improved T_2 contrast abilities over the individual IONPs. These particles were proposed as a candidate for mapping brain activity, because changes in Ca^{2+} concentration are indicative of synaptic activity [46].
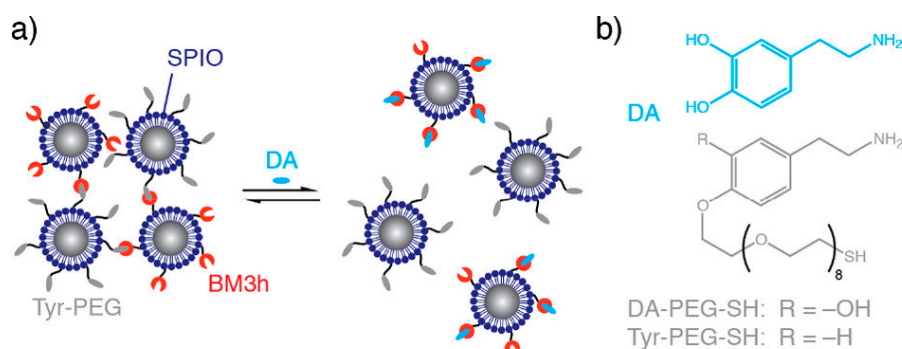
Figure 4. Dopamine sensitive IONPs. (**a**) The effect of dopamine on particle aggregation. In the absence of dopamine, nanocluster assemblies form owing to binding between protein (BM3h) and a dopamine analogue (Tyr-PEG). On addition of dopamine (DA), competitive binding inhibits self-assembly. (**b**) The structures of dopamine and tethered dopamine analogue. Reprinted (adapted) with permission from the authors of [11]. Copyright (2019) American Chemical Society.

3.3. Protein-Responsive

A subset of biomolecule-responsive contrast agents are those that have the ability to respond to a specific protein, a potent potential asset in, for example, cancer diagnostics, where tumour growth is often associated with an overexpression of potential marker proteins [47,48]. In proof of principal work, protein recognition has been achieved with biotin surface modified, Gd-doped MSNs, reversibly switching T_1 contrast through a reversible steric capping of the pore channels with streptavidin [39]. On binding streptavidin, successful capping of the pore channel was achieved, inhibiting diffusive water access to the internal paramagnetic chelates and rendering low relaxivity. In the presence of excess biotin in solution, streptavidin was observed to be competed off the surface of the particle, restoring water access and high relaxivity.

The role of enzymes in biological and metabolic conditions is also well established, where the presence of specific forms can be associated with a range of pathological conditions, for example, cancer, inflammation, or neurodegeneration [49–51]. Often, enzyme-responsive contrast systems contain cleavable linkages that alter the relaxometric properties of the nanoparticulate platform. One such example is the sensing of matrix metalloproteinase (MMP) enzymes by IONPs [52]. In this work, two different particles were produced, one functionalised with azide groups, and the other with alkyne groups, with both containing peptide sequences that have the ability to target the specific tumour site. In the presence of MMP enzymes, the peptide sequence is cleaved, exposing the alkyne/azide groups on the particles, facilitating a "click" reaction between the two, forming nanocluster assemblies. These display a greater saturation magnetisation than the individual IONPs, accompanied with a 160% increase in T_2 activity (Figure 5). Alternatively, nanoparticles with the ability to mimic enzymatic activity, in particular MnO nanoparticles that are able to imitate superoxide dismutase (SOD) enzymes, have recently been reported [53]. Tumour tissues often show elevated concentrations of superoxide radicals, as the enzyme responsible for regulating their level, SOD, is present in lower quantities within the cells. The MnO particles were observed to be reduced by the superoxide radicals, inducing a decrease in the electronic spin of the metal ion, and thus a longer relaxation time.

Table 1. A summary of the bio-responsive magnetic nanoparticulate systems encompassed in this review. The sizes, changes in relaxivity, stimulus, as well as the advantages of each sytem are included. MMP, matrix metalloproteinase; PAA, poly(acrylic acid); MSN, mesoporous silica nanoparticle; MRI, magnetic resonance imaging; GSH, glutathione.

Type	Size	Relaxivities	Stimulus	Advantages	Reference
Hydrazine cross linked iron oxide nanocluster assemblies	Iron Oxide Nanoparticles = 9 nm, Nanocluster = 60 nm	r_2/r_1 = 4.2 at pH 5.5, r_2/r_1 = 33.8 at pH 7.4	pH	T_1/T_2 switch in contrast capabilities	[25]
Fe_3O_4-ZIF-8 assemblies	Iron Oxide Nanoparticles = 15 nm, Fe_3O_4-ZIF-8 = 120 nm	r_2/r_1 = 5.7 at pH 5.0, r_2/r_1 = 24.6 at pH 7.4	pH, GSH (redox)	T_1/T_2 switch in contrast capabilities	[30]
i-motif DNA-assisted iron oxide nanocluster assemblies (RIAs)	Iron Oxide Nanoparticles ~3 nm, RIAs = 120 nm	r_2/r_1 = 7.1 at pH 5.5, r_2/r_1 = 63.3 at pH 7.4	pH	T_1/T_2 switch in contrast capabilities	[31]
pH sensitive 'magnetic nanogrenades' (PMNs)	Iron Oxide Nanoparticles ~3 nm, PMNs ~60 nm	r_2/r_1 = 5.8 at pH 5.5, r_2/r_1 = 13.3 at pH 7.4	pH	T_1/T_2 switch in contrast capabilities	[32]
Biotin surface modified Gd-doped MSNs	75 ± 6 nm	Native MSNs r_1 = 15.1 mM^{-1} s^{-1}, Biocapped MSNs r_1 = 5.8 mM^{-1} s^{-1}	Biotin	Reversible protein recognition	[39]
Gd-MSNs-PgPAA	61 ± 8 nm	r_1 = 8.7 mM^{-1} s^{-1} at pH 4.0, r_1 = 20.1 mM^{-1} s^{-1} at pH 7.0	pH	Fully reversible T_1 contrast switch	[40]
MnOx integrated hollow MSNs	~240 nm	r_1 = 8.8 mM^{-1} s^{-1} at pH 5.0, r_1 = 0.8 mM^{-1} s^{-1} at pH 7.4	pH	Multimodal imaging agent (MRI and US)	[41]
Fe_3O_4@C@MnO_2	130 nm	r_2/r_1 = 68.7 at pH 5.0, r_2/r_1 = 201.1 at pH 7.4	pH	Dual-modal T_1/T_2 contrast agent	[42]
Dopamine-responsive IONPs (DaReNa, SPIO = superparamagnetic iron oxide)	DaReNa = 138 ± 4 nm, 9D7*-SPIO = 52 ± 2 nm, Tyr-PEG-SPIO = 31 ± 1 nm	r_2 = 208 ± 2 mM^{-1} s^{-1} (DaReNa), r_2 = 130–140 mM^{-1} s^{-1} individual IONP species	Dopamine	Neurochemistry unaffected	[11]
Calcium-responsive nanoparticles (MaCaReNas)	35 ± 1 nm in absence of Ca^{2+}, 262 ± 14 nm in presence of Ca^{2+}	r_2 = 151 ± 15 mM^{-1} s^{-1} with 0 mM Ca^{2+}, r_2 = 261 ± 21 mM^{-1} s^{-1} with 1.2 mM Ca^{2+}	Calcium	Allows for calcium activity mapping in the brain	[46]
MMP-responsive iron oxide nanoparticles	Azide IONPs = 120 ± 8 nm, Alkyne IONPs = 148 ± 10 nm, presence of MMP enzymes = 780 nm	T_2 signal enhancement of ~160%	Matrix metalloproteinase enzymes	Tumour-targeting contrast agent	[52]
Manganese oxide nanoparticles	8 ± 0.7 nm	r_2/r_1 = 14.1 in absence of superoxide radicals, r_2/r_1 = 31.7 in the presence of superoxide radicals	Superoxide radicals	Can mimic the enzyme superoxide dismutase, thus catalyse the dismutation of superoxide radicals	[53]
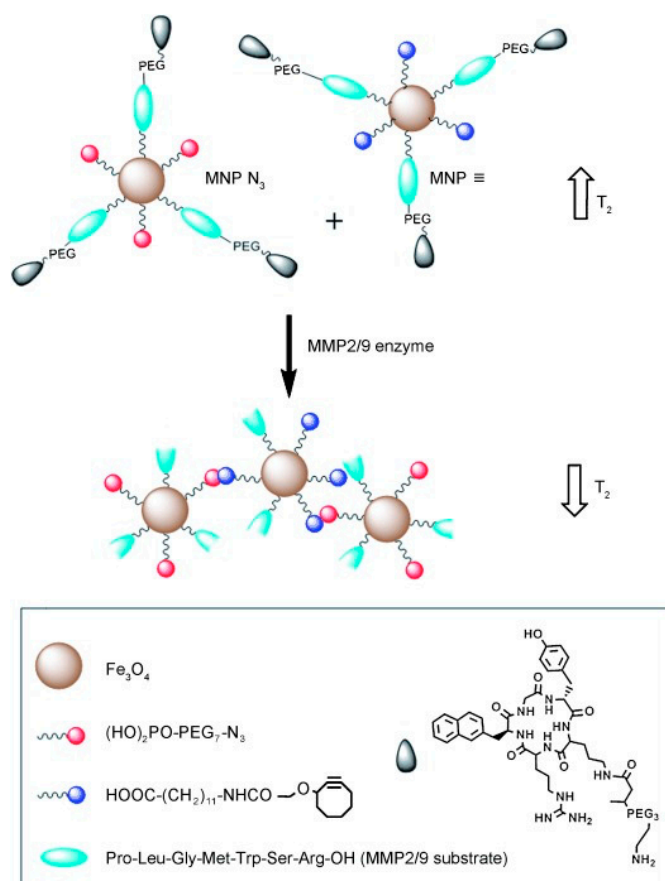
Figure 5. A schematic representing the click coupling of IONPs functionalised with azide (red) groups and those functionalised with alkyne groups (blue). These particles expose azide/alkyne groups in the prescence of matrix metalloproteinase (MMP) enzymes, facilitating a click reaction mediated particle coupling. The effect on the T_2 relaxation can be seen alongside both the individual IONPs (top) and the nanocluster (bottom). The particles also contain tumour specific peptide ligands and are functionalised with PEG to improve biocompatibility *in vivo*. Reprinted with permission from the authors of [52]. Copyright (2014), with permission from John Wiley and Sons.

4. Conclusions and Future Outlook

Nanoparticulate MR contrast agents offer improved blood circulation times and markedly greater relaxivities compared with molecular analogues, and can be readily designed to integrate both additional imaging modes and a responsive drug delivery capability. By further introducing bio-responsivity, these become more potent still and one can foresee their use becoming ever more prevalent in early identification of disease. This bio-responsivity arises from the chemists' ability to understand and tune characteristics that govern relaxivity; for example, the manipulation of diffusive water access to magnetic centres or of rotational motion by controlling aggregation. Within this short review, nanoparticles with pH-, enzyme-, molecular-, ion-, and protein-responsive properties have all been discussed and exemplified with recent works. Despite much progress during the past decade, there remains an enormous scope to advance this field, with a plethora of physiological conditions that could be investigated. One potentially fruitful organic–inorganic marriage is, for example, the integration of thermo-responsive polymers with paramagnetic/superparamagnetic metal hosting particle architectures. These polymers can mediate a significant change in hydration and solubility with changes in temperature [54–56], and have been applied to thermo-responsive drug release [57–60]. The integration of an associated high resolution imaging mode, such as MR, would also facilitate a direct imaging of treatment efficacy by magnetic hyperthermia. In addition, the versatility of nanoparticulate

platforms provides scope to introduce additional imaging modalities, such as the incorporation of radiotracers to produce dual-modal PET/MR-responsive agents. MSNs represent one such promising platform, as amino anchor groups can be introduced with relative ease, facilitating a broad range of subsequent functionalities to be tethered. Furthermore, therapeutic agents can be loaded within porous or hollow particles such as these and thus produce a potent multimodal, bio-responsive theranostic agent. The application of engineerable platforms such as this could revolutionalise the way disease states are diagnosed, monitored, and treated.

References

1. Shin, T.-H.; Choi, Y.; Kim, S.; Cheon, J. Recent advances in magnetic nanoparticle-based multi-modal imaging. *Chem. Soc. Rev.* **2015**, *44*, 4501–4516. [CrossRef]
2. Ni, D.; Bu, W.; Ehlerding, E.B.; Cai, W.; Shi, J. Engineering of inorganic nanoparticles as magnetic resonance imaging contrast agents. *Chem. Soc. Rev.* **2017**, *46*, 7438–7468. [CrossRef]
3. Gobbo, O.L.; Sjaastad, K.; Radomski, M.W.; Volkov, Y.; Prina-Mello, A. Magnetic nanoparticles in cancer theranostics. *Theranostics* **2015**, *5*, 1249. [CrossRef]
4. Singh, A.; Sahoo, S.K. Magnetic nanoparticles: A novel platform for cancer theranostics. *Drug Discov. Today* **2014**, *19*, 474–481. [CrossRef]
5. Pellico, J.; Ellis, C.M.; Davis, J.J. Nanoparticle-Based Paramagnetic Contrast Agents for Magnetic Resonance Imaging. *Contrast Media Mol. Imaging* **2019**, *2019*, 13. [CrossRef]
6. Angelovski, G. What We Can Really Do with Bioresponsive MRI Contrast Agents. *Angew. Chem. Int. Ed.* **2016**, *55*, 7038–7046. [CrossRef]
7. Liu, R.; Liao, P.; Liu, J.; Feng, P. Responsive Polymer-Coated Mesoporous Silica as a pH-Sensitive Nanocarrier for Controlled Release. *Langmuir* **2011**, *27*, 3095–3099. [CrossRef]
8. Popat, A.; Liu, J.; Lu, G.Q.; Qiao, S.Z. A pH-responsive drug delivery system based on chitosan coated mesoporous silica nanoparticles. *J. Mater. Chem.* **2012**, *22*, 11173–11178. [CrossRef]
9. Peng, H.; Dong, R.; Wang, S.; Zhang, Z.; Luo, M.; Bai, C.; Zhao, Q.; Li, J.; Chen, L.; Xiong, H. A pH-responsive nano-carrier with mesoporous silica nanoparticles cores and poly(acrylic acid) shell-layers: Fabrication, characterization and properties for controlled release of salidroside. *Int. J. Pharm.* **2013**, *446*, 153–159. [CrossRef]
10. Bilalis, P.; Tziveleka, L.-A.; Varlas, S.; Iatrou, H. pH-Sensitive nanogates based on poly(l-histidine) for controlled drug release from mesoporous silica nanoparticles. *Polym. Chem.* **2016**, *7*, 1475–1485. [CrossRef]
11. Hsieh, V.; Okada, S.; Wei, H.; García-Álvarez, I.; Barandov, A.; Recuenco Alvarado, S.; Ohlendorf, R.; Fan, J.; Ortega, A.; Jasanoff, A. Neurotransmitter-responsive nanosensors for T2-weighted magnetic resonance imaging. *J. Am. Chem. Soc.* **2019**, *141*, 15751–15754. [CrossRef] [PubMed]
12. Lu, Y.; Aimetti, A.A.; Langer, R.; Gu, Z. Bioresponsive materials. *Nat. Rev. Mater.* **2016**, *2*, 16075. [CrossRef]
13. Viger, M.L.; Sankaranarayanan, J.; de Gracia Lux, C.; Chan, M.; Almutairi, A. Collective Activation of MRI Agents via Encapsulation and Disease-Triggered Release. *J. Am. Chem. Soc.* **2013**, *135*, 7847–7850. [CrossRef]
14. Wahsner, J.; Gale, E.M.; Rodríguez-Rodríguez, A.; Caravan, P. Chemistry of MRI Contrast Agents: Current Challenges and New Frontiers. *Chem. Rev.* **2019**, *119*, 957–1057. [CrossRef]
15. Davies, G.-L.; Kramberger, I.; Davis, J.J. Environmentally responsive MRI contrast agents. *Chem. Commun.* **2013**, *49*, 9704–9721. [CrossRef]
16. Que, E.L.; Chang, C.J. Responsive magnetic resonance imaging contrast agents as chemical sensors for metals in biology and medicine. *Chem. Soc. Rev.* **2010**, *39*, 51–60. [CrossRef]
17. Sherry, A.D.; Wu, Y. The importance of water exchange rates in the design of responsive agents for MRI. *Curr. Opin. Chem. Biol.* **2013**, *17*, 167–174. [CrossRef]

18. Caravan, P.; Ellison, J.J.; McMurry, T.J.; Lauffer, R.B. Gadolinium(III) Chelates as MRI Contrast Agents: Structure, Dynamics, and Applications. *Chem. Rev.* **1999**, *99*, 2293–2352. [CrossRef]

19. Dennis, A.M.; Rhee, W.J.; Sotto, D.; Dublin, S.N.; Bao, G. Quantum Dot–Fluorescent Protein FRET Probes for Sensing Intracellular pH. *ACS Nano* **2012**, *6*, 2917–2924. [CrossRef]

20. Wu, Z.L.; Gao, M.X.; Wang, T.T.; Wan, X.Y.; Zheng, L.L.; Huang, C.Z. A general quantitative pH sensor developed with dicyandiamide N-doped high quantum yield graphene quantum dots. *Nanoscale* **2014**, *6*, 3868–3874. [CrossRef]

21. Song, Y.; Li, Y.; Xu, Q.; Liu, Z. Mesoporous silica nanoparticles for stimuli-responsive controlled drug delivery: Advances, challenges, and outlook. *Int. J. Nanomed.* **2017**, *12*, 87. [CrossRef]

22. Sonawane, S.J.; Kalhapure, R.S.; Govender, T. Hydrazone linkages in pH responsive drug delivery systems. *Eur. J. Pharm. Sci.* **2017**, *99*, 45–65. [CrossRef]

23. Dai, Y.; Xu, C.; Sun, X.; Chen, X. Nanoparticle design strategies for enhanced anticancer therapy by exploiting the tumour microenvironment. *Chem. Soc. Rev.* **2017**, *46*, 3830–3852. [CrossRef] [PubMed]

24. Mura, S.; Nicolas, J.; Couvreur, P. Stimuli-responsive nanocarriers for drug delivery. *Nat. Mater.* **2013**, *12*, 991. [CrossRef] [PubMed]

25. Li, F.; Liang, Z.; Liu, J.; Sun, J.; Hu, X.; Zhao, M.; Liu, J.; Bai, R.; Kim, D.; Sun, X.; et al. Dynamically Reversible Iron Oxide Nanoparticle Assemblies for Targeted Amplification of T1-Weighted Magnetic Resonance Imaging of Tumors. *Nano Lett.* **2019**, *19*, 4213–4220. [CrossRef]

26. Kaittanis, C.; Shaffer, T.M.; Ogirala, A.; Santra, S.; Perez, J.M.; Chiosis, G.; Li, Y.; Josephson, L.; Grimm, J. Environment-responsive nanophores for therapy and treatment monitoring via molecular MRI quenching. *Nat. Commun.* **2014**, *5*, 3384. [CrossRef]

27. Na, H.B.; Song, I.C.; Hyeon, T. Inorganic Nanoparticles for MRI Contrast Agents. *Adv. Mater.* **2009**, *21*, 2133–2148. [CrossRef]

28. Wei, H.; Bruns, O.T.; Kaul, M.G.; Hansen, E.C.; Barch, M.; Wiśniowska, A.; Chen, O.; Chen, Y.; Li, N.; Okada, S.; et al. Exceedingly small iron oxide nanoparticles as positive MRI contrast agents. *Proc. Natl. Acad. Sci. USA* **2017**, *114*, 2325–2330. [CrossRef]

29. Pellico, J.; Ruiz-Cabello, J.; Fernández-Barahona, I.; Gutiérrez, L.; Lechuga-Vieco, A.V.; Enríquez, J.A.; Morales, M.P.; Herranz, F. One-Step Fast Synthesis of Nanoparticles for MRI: Coating Chemistry as the Key Variable Determining Positive or Negative Contrast. *Langmuir* **2017**, *33*, 10239–10247. [CrossRef]

30. Lin, J.; Xin, P.; An, L.; Xu, Y.; Tao, C.; Tian, Q.; Zhou, Z.; Hu, B.; Yang, S. Fe3O4–ZIF-8 assemblies as pH and glutathione responsive T2–T1 switching magnetic resonance imaging contrast agent for sensitive tumor imaging in vivo. *Chem. Commun.* **2019**, *55*, 478–481. [CrossRef]

31. Lu, J.; Sun, J.; Li, F.; Wang, J.; Liu, J.; Kim, D.; Fan, C.; Hyeon, T.; Ling, D. Highly Sensitive Diagnosis of Small Hepatocellular Carcinoma Using pH-Responsive Iron Oxide Nanocluster Assemblies. *J. Am. Chem. Soc.* **2018**, *140*, 10071–10074. [CrossRef] [PubMed]

32. Ling, D.; Park, W.; Park, S.-J.; Lu, Y.; Kim, K.S.; Hackett, M.J.; Kim, B.H.; Yim, H.; Jeon, Y.S.; Na, K.; et al. Multifunctional Tumor pH-Sensitive Self-Assembled Nanoparticles for Bimodal Imaging and Treatment of Resistant Heterogeneous Tumors. *J. Am. Chem. Soc.* **2014**, *136*, 5647–5655. [CrossRef] [PubMed]

33. Stöber, W.; Fink, A.; Bohn, E. Controlled growth of monodisperse silica spheres in the micron size range. *J. Colloid Interface Sci.* **1968**, *26*, 62–69. [CrossRef]

34. Kresge, C.T.; Leonowicz, M.E.; Roth, W.J.; Vartuli, J.C.; Beck, J.S. Ordered mesoporous molecular sieves synthesized by a liquid-crystal template mechanism. *Nature* **1992**, *359*, 710–712. [CrossRef]

35. Zhou, Y.; Quan, G.; Wu, Q.; Zhang, X.; Niu, B.; Wu, B.; Huang, Y.; Pan, X.; Wu, C. Mesoporous silica nanoparticles for drug and gene delivery. *Acta Pharm. Sin. B* **2018**, *8*, 165–177. [CrossRef] [PubMed]

36. Wang, Y.; Zhao, Q.; Han, N.; Bai, L.; Li, J.; Liu, J.; Che, E.; Hu, L.; Zhang, Q.; Jiang, T.; et al. Mesoporous silica nanoparticles in drug delivery and biomedical applications. *Nanomed. Nanotechnol. Biol. Med.* **2015**, *11*, 313–327. [CrossRef]

37. Tang, F.; Li, L.; Chen, D. Mesoporous Silica Nanoparticles: Synthesis, Biocompatibility and Drug Delivery. *Adv. Mater.* **2012**, *24*, 1504–1534. [CrossRef]

38. Davis, J.J.; Huang, W.-Y.; Davies, G.-L. Location-tuned relaxivity in Gd-doped mesoporous silica nanoparticles. *J. Mater. Chem.* **2012**, *22*, 22848–22850. [CrossRef]

39. Huang, W.-Y.; Davies, G.-L.; Davis, J.J. High signal contrast gating with biomodified Gd doped mesoporous nanoparticles. *Chem. Commun.* **2013**, *49*, 60–62. [CrossRef]

40. Pellico, J.; Ellis, C.M.; Miller, J.; Davis, J.J. Water gated contrast switching with polymer–silica hybrid nanoparticles. *Chem. Commun.* **2019**, *55*, 8540–8543. [CrossRef]

41. Chen, Y.; Yin, Q.; Ji, X.; Zhang, S.; Chen, H.; Zheng, Y.; Sun, Y.; Qu, H.; Wang, Z.; Li, Y.; et al. Manganese oxide-based multifunctionalized mesoporous silica nanoparticles for pH-responsive MRI, ultrasonography and circumvention of MDR in cancer cells. *Biomaterials* **2012**, *33*, 7126–7137. [CrossRef] [PubMed]

42. Duan, B.; Wang, D.; Wu, H.; Xu, P.; Jiang, P.; Xia, G.; Liu, Z.; Wang, H.; Guo, Z.; Chen, Q. Core–Shell Structurized Fe_3O_4@C@MnO_2 Nanoparticles as pH Responsive T1-T2* Dual-Modal Contrast Agents for Tumor Diagnosis. *ACS Biomater. Sci. Eng.* **2018**, *4*, 3047–3054. [CrossRef]

43. Li, W.-H.; Fraser, S.E.; Meade, T.J. A Calcium-Sensitive Magnetic Resonance Imaging Contrast Agent. *J. Am. Chem. Soc.* **1999**, *121*, 1413–1414. [CrossRef]

44. Major, J.L.; Boiteau, R.M.; Meade, T.J. Mechanisms of ZnII-Activated Magnetic Resonance Imaging Agents. *Inorg. Chem.* **2008**, *47*, 10788–10795. [CrossRef]

45. Luo, Y.; Kim, E.H.; Flask, C.A.; Clark, H.A. Nanosensors for the Chemical Imaging of Acetylcholine Using Magnetic Resonance Imaging. *ACS Nano* **2018**, *12*, 5761–5773. [CrossRef]

46. Okada, S.; Bartelle, B.B.; Li, N.; Breton-Provencher, V.; Lee, J.J.; Rodriguez, E.; Melican, J.; Sur, M.; Jasanoff, A. Calcium-dependent molecular fMRI using a magnetic nanosensor. *Nat. Nanotechnol.* **2018**, *13*, 473–477. [CrossRef]

47. Liu, Z.; Wang, F.; Chen, X. Integrin αvβ3-targeted cancer therapy. *Drug Dev. Res.* **2008**, *69*, 329–339. [CrossRef]

48. Herbst, R.S. Review of epidermal growth factor receptor biology. *Int. J. Radiat. Oncol. Biol. Phys.* **2004**, *59*, 21–26. [CrossRef]

49. Wang, X.; Wang, X.; Jin, S.; Muhammad, N.; Guo, Z. Stimuli-Responsive Therapeutic Metallodrugs. *Chem. Rev.* **2019**, *119*, 1138–1192. [CrossRef]

50. Hu, Q.; Katti, P.S.; Gu, Z. Enzyme-responsive nanomaterials for controlled drug delivery. *Nanoscale* **2014**, *6*, 12273–12286. [CrossRef]

51. Zhang, H.-W.; Wang, L.-Q.; Xiang, Q.-F.; Zhong, Q.; Chen, L.-M.; Xu, C.-X.; Xiang, X.-H.; Xu, B.; Meng, F.; Wan, Y.-Q.; et al. Specific lipase-responsive polymer-coated gadolinium nanoparticles for MR imaging of early acute pancreatitis. *Biomaterials* **2014**, *35*, 356–367. [CrossRef] [PubMed]

52. Gallo, J.; Kamaly, N.; Lavdas, I.; Stevens, E.; Nguyen, Q.-D.; Wylezinska-Arridge, M.; Aboagye, E.O.; Long, N.J. CXCR4-Targeted and MMP-Responsive Iron Oxide Nanoparticles for Enhanced Magnetic Resonance Imaging. *Angew. Chem. Int. Ed.* **2014**, *53*, 9550–9554. [CrossRef] [PubMed]

53. Ragg, R.; Schilmann, A.M.; Korschelt, K.; Wieseotte, C.; Kluenker, M.; Viel, M.; Völker, L.; Preiß, S.; Herzberger, J.; Frey, H.; et al. Intrinsic superoxide dismutase activity of MnO nanoparticles enhances the magnetic resonance imaging contrast. *J. Mater. Chem. B* **2016**, *4*, 7423–7428. [CrossRef]

54. Wei, M.; Gao, Y.; Li, X.; Serpe, M.J. Stimuli-responsive polymers and their applications. *Polym. Chem.* **2017**, *8*, 127–143. [CrossRef]

55. Klouda, L. Thermoresponsive hydrogels in biomedical applications: A seven-year update. *Eur. J. Pharm. Biopharm.* **2015**, *97*, 338–349. [CrossRef]

56. Hoffman, A.S.; Stayton, P.S. Conjugates of stimuli-responsive polymers and proteins. *Prog. Polym. Sci.* **2007**, *32*, 922–932. [CrossRef]

57. Purushotham, S.; Chang, P.; Rumpel, H.; Kee, I.; Ng, R.; Chow, P.; Tan, C.; Ramanujan, R. Thermoresponsive core–shell magnetic nanoparticles for combined modalities of cancer therapy. *Nanotechnology* **2009**, *20*, 305101. [CrossRef]

58. Yar, Y.; Khodadust, R.; Akkoc, Y.; Utkur, M.; Saritas, E.U.; Gozuacik, D.; Yagci Acar, H. Development of tailored SPION-PNIPAM nanoparticles by ATRP for dually responsive doxorubicin delivery and MR imaging. *J. Mater. Chem. B* **2018**, *6*, 289–300. [CrossRef]

59. Rastogi, R.; Gulati, N.; Kotnala, R.K.; Sharma, U.; Jayasundar, R.; Koul, V. Evaluation of folate conjugated pegylated thermosensitive magnetic nanocomposites for tumor imaging and therapy. *Colloids Surf. B Biointerfaces* **2011**, *82*, 160–167. [CrossRef]

60. Li, Q.; Zhang, L.; Bai, L.; Zhang, Z.; Zhu, J.; Zhou, N.; Cheng, Z.; Zhu, X. Multistimuli-responsive hybrid nanoparticles with magnetic core and thermoresponsive fluorescence-labeled shell via surface-initiated RAFT polymerization. *Soft Matter* **2011**, *7*, 6958–6966. [CrossRef]